Analysis of Squirrel Cage Effect in Single Phase LSPM

Byung-Taek Kim†, Young-Kwan Kim* and Duk-Jin Kim*

Abstract - This paper presents the analysis of the effects of non-uniform slots in a line start permanent magnet (LSPM) motor. For purposes of the investigation, the simple formula of 2nd resistance for rotors having different slot areas is deduced. The characteristic analysis using the formula is performed and compared with measurement results.

Keywords: line start permanent magnet motor, squirrel cage, single phase induction motor

1. Introduction

As saving energy becomes a world-wide issue, the efficiency of electric machines for use in home appliances becomes increasingly important. With this focus, the 1-phase induction motor is being replaced with the permanent magnet type motor because of its improved characteristics and decrease in the cost of permanent magnet material. The most popular motor using permanent magnet material is the brushless DC motor, but it also requires use of a high cost inverter. So the single-phase line start permanent magnet (LSPM) motor is being studied as an alternative to the induction motor [1, 2]. The rotor of the 1-phase LSPM has both the permanent magnet and squirrel cage. Therefore it can start without inverter assistance, such as in the case of the induction motor and furthermore, it shows the performance of the synchronous motor after synchronization. Generally, the d-q equivalent circuit is used for analysis of the 1-phase LSPM. In the analysis, the accuracy of the circuit parameters, especially the 2nd resistance of the rotor circuit, is very important because it influences largely upon the abilities to start and synchronize [3].

The general shapes of the rotor bars and end-ring of the LSPM are non-uniform and complex because there must be some permanent magnets and flux barriers in the rotor. So the conventional formula cannot be applied for obtaining the accurate parameter of rotor circuit, that is, 2nd resistance.

This paper details the effects on the starting and synchronization characteristics according to the squirrel cage of the rotor. For accurate analysis, the method of calculating the 2nd resistance of the rotor circuit is deduced. The proposed system is able to consider the non-uniform shape of the rotor bars. The characteristic analysis is performed using the obtained parameters and then compared with the test results.

† Corresponding author: Digital Appliance Research Laboratory, LG Electronics Inc, Seoul, Korea (kbtcej@lge.com)
* Digital Appliance Research Laboratory, LG Electronics Inc, Seoul, Korea
Received May 6, 2004 ; Accepted October 22, 2004

2. Analysis Method

2.1 Analysis Model

Fig. 1 shows the analysis model of the LSPM motor. Each slot of the model has a different shape and area. The structure was designed for minimizing the leakage flux from the magnet and maximizing the ratio of Ld and Lq. The specification and the areas of rotor slots of the model are presented in Table 1.

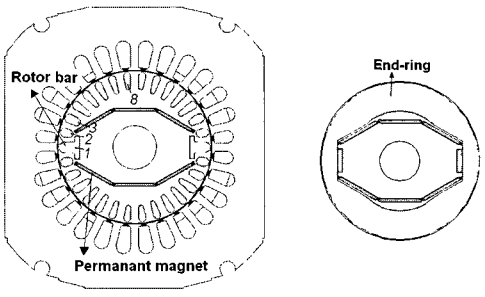

(a) Stator and rotor (b) End-ring

Fig. 1 Analysis model

Table 1 Specification of analysis model

General specification				Slot area [mm²]	
Item	Value	Item	Value	No.	Area
Air-gap	0.5mm	Mag.	NdFeB	1	47
Rm	19.4Ω	Vol.	220V	2,8	18
Ra	20. Ω	Cs	45uF	3	22
Na/Nm	0.82	Cr	2uF	4	25
Din	62mm	Freq.	50Hz	5~7	21

2.2 Rotor Modeling

The formula for rotor resistance for the general induction motor is given by (1). In the equation, S_r is the number of rotor slots and L_b, D_{er}, a_b and a_{er} is bar length, diameter of end-ring, areas of bar and end-ring, respectively. In the formula, it is assumed that every rotor bar has the identical shape and area so that the distribution of bar currents is sinusoidal in the periphery of the rotor [4].

$$R_r = \rho S_r^2 \left\{ \frac{L_b}{S_r a_b} + \frac{2D_{er}}{\pi P a_{er}} \right\} \tag{1}$$

The LSPM motor for analysis has non-uniform slot shapes and areas. It creates non-sinusoidal bar currents and non-uniform bar resistances. As such, detailed calculation of 2nd resistance is needed for precise analysis. The rotor shape and the equivalent circuit model for the calculation of resistance are presented in Fig. 2 [5]. In the figure, minor loop's EMF of rotor circuit, e_n is given by (2), where $\hat{e}$ is maximum value of the EMF. Also the EMF can be represented by Kirchhoff's voltage law and given by (3).

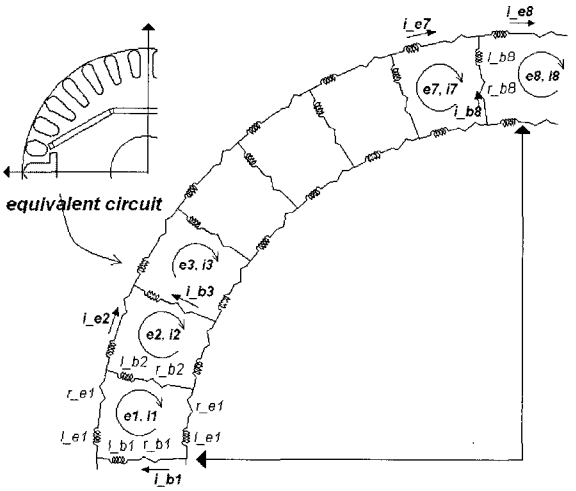

Fig. 2 Modeling of rotor circuit

$$e_n = \hat{e}\cos(\omega t - (2\pi/S_r)n), \quad n = 1,2,..,S_r \tag{2}$$

$$e_n = (r_{bn} + r_{bn+1} + 2r_{en})i_n + (l_{bn} + l_{bn+1} + 2l_{en})\frac{di_n}{dt} \tag{3}$$

The second term of (3) can be assumed to be small compared with the resistive term, especially at high rotor speed, so the equation is approximated as (4).

$$e_n \approx (r_{bn} + r_{bn+1} + 2r_{en})i_n \tag{4}$$

The voltage equations for rotor circuit are represented by (5).

$$\begin{aligned} e_0 &= (r_{b2} + r_{b1} + 2r_{e1})i_0, \quad r_{b0} = r_{b2} \\ e_1 &= (r_{b1} + r_{b2} + 2r_{e1})i_1 \\ &\cdot \\ &\cdot \\ e_8 &= (r_{b8} + r_{b8} + 2r_8)i_8, \quad r_{b9} = r_{b8} \end{aligned} \tag{5}$$

Using (5), the end-ring current and the bar current are generalized by (6) and (7), respectively.

$$i_{en} = i_n = \frac{e_n}{(r_{bn} + r_{bn+1} + 2r_{e1})} = \hat{e}k_n, \tag{6}$$

$$i_{bn} = i_n - i_{n-1} = \hat{e}(k_n - k_{n-1}) \tag{7}$$

$$\text{, where } k_n = \frac{\cos(\omega t - (2\pi/S_r)n))}{(r_{bn} + r_{bn+1} + 2r_{en})}. \tag{8}$$

Elementary copper loss in the end-ring and bar can be obtained using (6) and (7), as in (9) and (10).

$$W_{bn} = (i_{bn})^2 r_{bn} = \hat{e}^2 (k_n - k_{n-1})^2 r_{bn} \tag{9}$$

$$W_{en} = (i_{en})^2 r_{en} = \hat{e}^2 (k_n)^2 r_{en} \tag{10}$$

The total copper loss in the rotor is given by (11) and can be replaced including geometry function, as shown in (12).

$$W_{rotor} = 2P \sum_{n=1}^{S_r/2P} (W_{bn} + W_{en}) \tag{11}$$

$$= 2P \sum_{n=1}^{S_r/2P} (i_{bn})^2 \left(r_{bn} + \left(\frac{k_n}{k_n - k_{n-1}} \right)^2 r_{en} \right) \tag{12}$$

Since the equivalent resistance is an effective value to represent the total loss when the fundamental current is flowing, the effective rotor resistance can be written as (13)

$$W_{rotor} = (I_{b\_fun})^2 R_{r\_eff} = (\hat{e}k'_{fun})^2 R_{r\_eff} \tag{13}$$

, where the subscript *fun* means fundamental component and k'_{fun} is the fundamental component of series function, $\sum_{n=1}^{S_r} k_n - k_{n-1}$, which signifies the normalized bar current. Using (12) and (13), the effective rotor resistance is

presented as,

$$R_{r\_eff} = \frac{2P\sum_{n=1}^{S_r/2P}\left((k_n - k_{n-1})^2 r_{bn} + (k_n)^2 r_{en}\right)}{(k'_{fun})^2} \quad (14)$$

However, equation (14) is deduced by approximation of (4), and it is more accurate than the conventional formula (1) for analysis of the LSPM motor. From (14), it could be known that the resistance, R_{r_eff} is a function of geometry and time, because k_n includes ωt in (8). This means that R_d is different with R_q. R_q can be obtained when $\omega t = \pi/S_r$, satisfying the following conditions.

$$e_0 = e_1 = \hat{e}\cos(4\pi / S_r), \quad i_{b1} = i_1 - i_0 = 0$$

And R_d can also be obtained when $\omega t = \pi/S_r - \pi/2$, so

$$e_0 = -e_1 = -\hat{e}\sin(4\pi / S_r).$$

2.3 Method of Characteristic Analysis

The single-phase LSPM motor can be analyzed using the d-q equivalent circuit. Because the motor circuit is composed with main and auxiliary windings, the voltage equation is transformed to the ideal 2-phase voltage equations using (15) and (16).

$$\bar{v}_a = v_{aux}, \quad \bar{v}_b = a v_{main} \quad (15)$$

$$\bar{i}_a = i_{aux}, \quad \bar{i}_b = \frac{1}{a} i_{main}, \quad (16)$$

, where turn ratio, $a = \frac{N_{aux}}{N_{main}}$

Using Park's transform, the d-q equations are obtained from 2-phase circuit equations, as follows.

$$v_d = (R_s + pL_d)i_d - \omega_r L_q i_q + pL_{md} i_{2d} - \omega_r L_{mq} i_{2q} + pL_{md} i_{fm} \quad (17)$$

$$v_q = \omega_r L_d i_d + (R_s + pL_q)i_q + \omega_r L_{md} i_{2q} + \omega_r L_{md} i_{fm} \quad (18)$$

$$0 = pL_{md} i_d + (R_d + pL_{2d})i_{2d} + pL_{md} i_{fm} \quad (19)$$

$$0 = pL_{mq} i_q + (R_q + pL_{2q})i_{2q} \quad (20)$$

The above differential equation can be solved with the following motion equation.

$$p\omega_r = \frac{P}{J}(T_e - T_L) \quad (21)$$

, where electromagnetic torque T_e is given by (22) in which T_L is load torque and J is rotor inertia.

$$T_e = 2P\{(L_d i_d + L_{md} i_{2d} + L_{md} i_{mf})i_q - (L_q i_q + L_{mq} i_{2q})i_d\} \quad (22)$$

3. Simulation Results

3.1 Parameter Extraction

3.1.1 R_d, R_q

Fig. 3 shows the plots of series function $\sum_{n=1}^{S_r} k_n - k_{n-1}$ for analysis model and those of rotor slots with average value of the model's total slot area. It is known that the bar currents are very sinusoidal in the case of the rotor with the same slots. But in the case of different slots, the bar currents are very non-sinusoidal, especially in the d-axis.

Using equation (14), R_d and R_q are obtained and shown in Fig. 4. They are compared using the conventional equation (1) in the figure. It shows R_d is quite larger than the resistance of identical rotor bars.

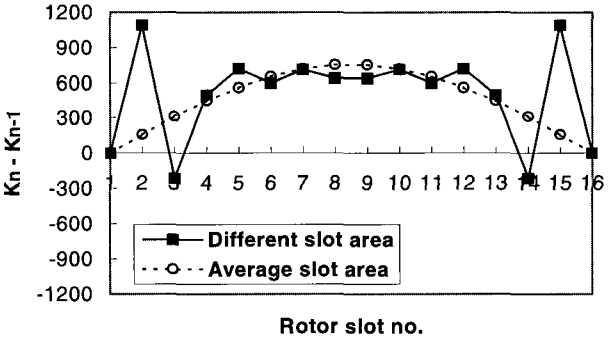

(a) Distribution of d-axis bar current

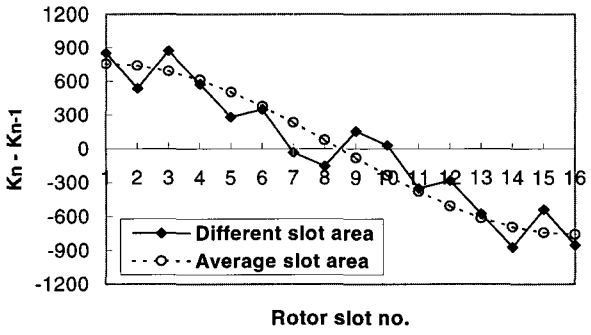

(b) Distribution of q-axis bar current

Fig. 3 Distribution of bar current

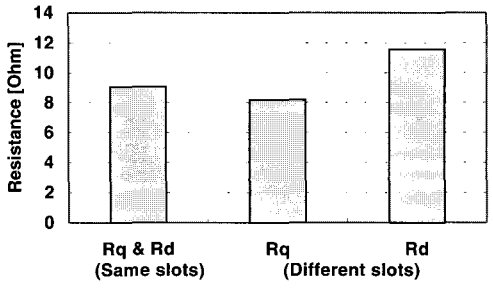

Fig. 4 Resistance of rotor

3.1.2 L_{md}, L_{mq} & i_{fm}

The magnetizing inductances according to d-q axis are obtained by calculation of flux linkage produced by stator current without magnet. For the calculation of flux linkage, FEA is carried out. Fig. 5 indicates the flux lines according to the flow of the d-q axis current. And the imaginary equivalent current representing magnet i_{fm} is determined by back EMF from a permanent magnet without other current sources, as shown in (23).

$$i_{fm} = \frac{E_0}{2\pi f L_{md}} \tag{23}$$

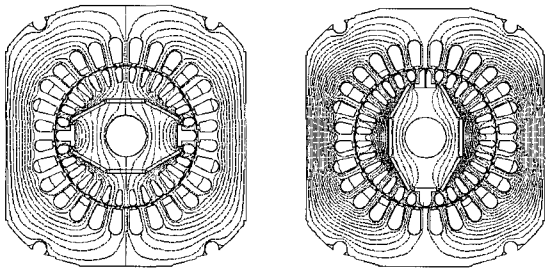

(a) d-axis (b) q-axis

Fig. 5 Flux lines according to d-q axis (using F.E.A)

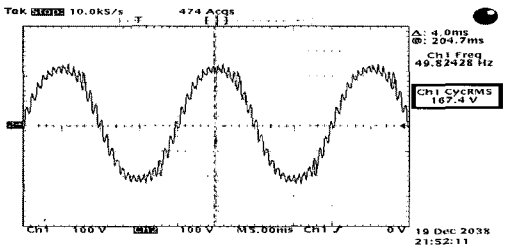

(a) Measurement result

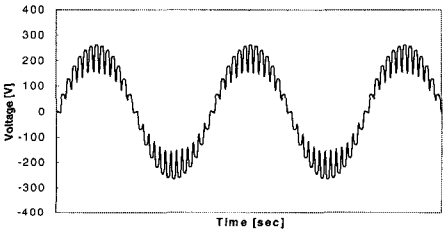

(b) Simulation result (using F.E.A)

Fig. 6 Back EMF in synchronous speed

Fig. 6 indicates the back EMF in auxiliary winding induced by the permanent magnet. The simulation results are in good agreement with the measurement results.

3.2 Steady & Transient State Performance

3.2.1 Steady state performance

The characteristics of the LSPM motor in steady state are not affected by resistance of rotor, because no electromotive force is induced in synchronous speed. So, the extracted parameter except for 2nd resistance can be verified by steady state analysis. The efficiency and the power factor are measured and the results are compared with simulation results in Fig. 7. There are very slight differences between them and it is known that the parameters are exceptionally accurate.

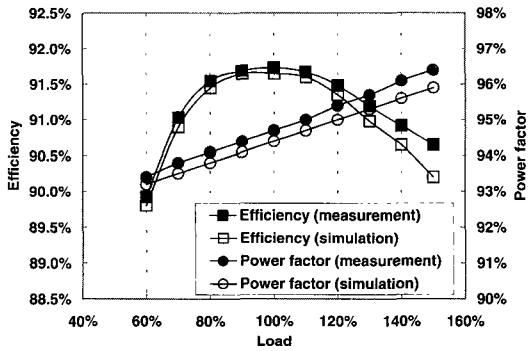

Fig. 7 Efficiency and power factor

3.2.2 Transient state performance

The single-phase LSPM motor is started and synchronized by induction torque and it works using magnet torque at synchronous speed. The characteristic analysis of the model prior to synchronization is performed by (17)~(22) according to variance of load torque. The characteristics of speed and torque are presented in Fig. 8. It shows that the motor having different slots is accelerated more rapidly than one having identical slots during low speeds. The reason can be explained by Fig. 9(a). It shows the starting torques of the motors without magnets for obtaining only induction torque. The simulation is performed for accounting the effect of the bar and with condition of $i_{fm} = \omega_r = p\omega_r = 0$ in derivative equations (17)~(20). The figure indicates that the average torque of the model having different slots is larger than that of the model having equivalent ones. The starting torque of the motor without a magnet is measured and the result is compared with simulation results in Fig. 9(b). The torque characteristics at the speed of $0.9\omega_s$ are analyzed and presented in Fig. 10. It can be shown that the two models have very large torque ripple and are almost identical. From the figure, it can be explained that the synchronization

times of the two motors are similar, despite rapid acceleration of the motor having different slots.

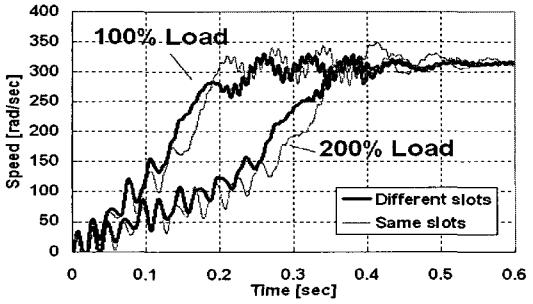

Fig. 8 Characteristics of speed and torque in transient state

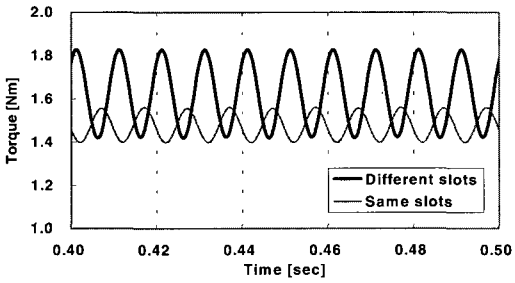

(a) Simulation of starting torque

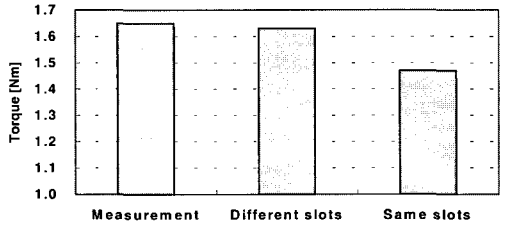

(b) Measurement of starting torque (average)

Fig. 9 Starting-torque of LSPM motor without magnet

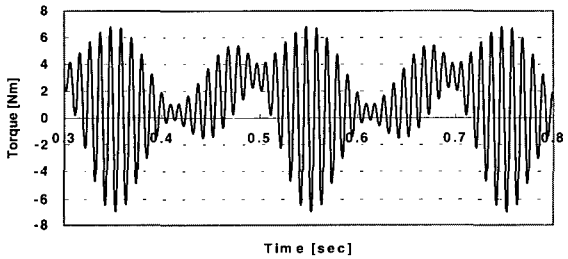

(a) Different slots

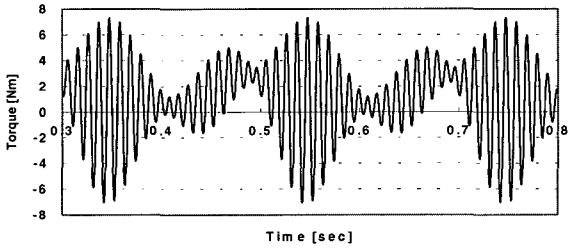

(b) Same slots

Fig. 10 Comparison of torque without magnet in high speed

4. Conclusion

In this paper, the simple formula for equivalent resistance of the bars having arbitrary slots is induced and applied to the analysis of the LSPM motor with a non-uniform rotor bar. Additionally the magnetizing inductance and back EMF are obtained using FEM for accurate analysis. From the analysis using the d-q equivalent circuit, it is known that the torque of the motor having non-uniform bar slots is larger at standstill but similar near synchronous speed, compared with the motor with identical slots of average area of non-uniform bar slots. This is helpful for purposes of design including load, inertia and PTC, etc.

References

[1] T. J. E. Miller, "Single phase permanent-magnet motor analysis", IEEE trans on Industrial application, Vol. IA-21, No. 4, pp. 651-658, May/June 1985.

[2] G. H Kang and J. P. Hong, "Analysis of single-phase line start-permanent synchronous motor", Trans KIEE, Vol. 50. No. 12, pp. 592-600 Dec 2001.

[3] T. J. E. Miller, "Synchronization of line-start permanent-magnet ac motor", IEEE trans on Power Apparatus and systems, Vol. PAS-103, No. 7, pp. 1822-1828, July 1984.

[4] E. S. Hamdi, Design of Small Electrical Machines, John Wiley & Sons, pp134, 1994.

[5] H. A. Toliyat, T. A. Lipo, "Transient analysis of cage induction machines under stator, rotor bar and end ring faults", IEEE trans on Energy conversion, Vol. 10, No. 2, pp 241-247, June 1995.

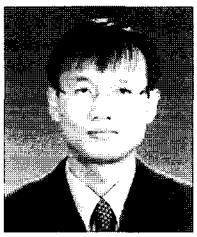

Byung-Taek Kim

He received B.S., M.S., and Ph.D. degrees in Electrical Engineering from Hanyang University, Korea, in 1994, 1996, and 2001, respectively. He is working as a Senior Researcher in the Digital Appliance Laboratory at LG Electronics Inc. His research interests include design of electric machines, numerical analysis, and optimization.

Young-Kwan Kim
He received B.S. and M.S. degrees in Electrical Engineering from Hanyang University, Korea, in 1990 and 1992, respectively. He is working as a Senior Researcher in the Digital Appliance Laboratory at LG Electronics Inc. His research interests include design of electric machines and numerical analysis.

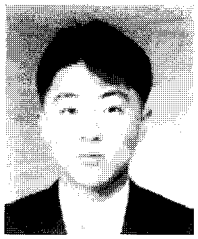

Duk-Jin Kim
He received B.S. and M.S. degrees in Electrical Engineering from Hanyang University, Korea, in 1998 and 2000, respectively. He is working as a Senior Researcher in the Digital Appliance Laboratory at LG Electronics Inc. His research interests include design of electric machines and numerical analysis.